

Comments on multiple scattering of high-energy muons in thick layers

A.V. Butkevich ^{a,*}, R.P. Kokoulin ^b, G.V. Matushko ^a and S.P. Mikheyev ^a

^a*Institute for Nuclear Research of Russian Academy of Science, 60th October Anniversary prospect, 7a, Moscow 117312, Russia.*

^b*Moscow State Engineering Physics Institute (Technical University), Kashirskoe Shosse, 31, Moscow 115409, Russia.*

Abstract

We describe two independent methods to calculate the angular distribution of muons after traversing a thick scatterer due to multiple Coulomb scattering. Both methods take into account the nuclear size effect. We demonstrate a necessity to account for the nucleus extension as well as incoherent scattering on atomic electrons to describe the muon scattering at large angles in thick matter layers. The results of the two methods of calculations are in good agreement.

PACS: 11.80.La; 25.30.Mr

Key words: Muon; Multiple Coulomb Scattering; Nuclear Size

* Corresponding author. Tel.: 07-095-334-0188; Fax: +07-095-334-0184.
Email address: butkevic@al20.inr.troitsk.ru (A.V. Butkevich).

1 Introduction

Multiple scattering of muons in the field of atoms is of interest for numerous applications related to muon transport in matter, in particular, for simulation of the response of high-energy particle detectors (including stochastic particle deviation in magnetized steel spectrometers), radiation protection tasks at accelerators, muon-induced background evaluations for cosmic ray neutrino experiments, etc. In many cases, reliable estimations of angular and lateral muon distribution functions at the level of probability of about $10^{-2} - 10^{-4}$ and lower are necessary. Furthermore, renewed interest to particle momentum evaluation on the basis of precise measurements of multiple scattering effect (utilising the scales and coordinate accuracies of novel muon and neutrino detectors) calls for adequate accuracies in the theoretical description of the phenomenon.

Several multiple scattering theories have been published (see review [1]) which are concerned with angular distribution of particles passing without substantial loss of energy $\Delta E \ll E$ using the small-angle approximation of scattering angle χ . This approximation assumes that χ is small and consists in replacing $\sin(\chi) \approx \tan(\chi) \approx \chi$ and the upper limit π for χ by infinity. Gaussian distribution function is widely used for various estimations, however it can hardly serve as a satisfactory tool for consideration of low probability region (large deflection angles), especially at moderate absorber thickness. On the other hand, Moliere theory [2],[3] of multiple scattering, the results of which are employed nowadays in most of the transport codes, cannot be used for description of high-energy muon scattering either. The reason is that, due to its large mass, muon is capable of passing large thicknesses of material, and hence the probability of scatters with impact parameters comparable with nuclear size is not small. Moliere theory (as well as other approaches developed within the point-like nucleus approximation) heavily overestimates the probability of large angle deflections.

Several calculations have been carried out to take into account the charge distribution in nucleus. Two methods [4] for evaluating multiple scattering on extended nuclei were given, one of which is of interest as a general method for any charge distribution. The expression for angular distribution was obtained in Ref.[5] under the assumption that the charge distribution in nuclei and proton is Gaussian. Unfortunately, there are several misprints in the work [5].

Moliere theory regarded elastic collisions against the screened Coulomb field of atomic nuclei only. Collisions with Z atomic electrons also contribute to multiple scattering, especially in light elements. This effect is often introduced by replacing Z^2 with $Z(Z + 1)$, which serves only to estimate the order of magnitude of the effect of inelastic scattering. The account of inelastic collisions in the Moliere theory has been done in Ref.[6] for electrons and heavy particles.

In this paper, we present two methods for calculation of the muon angular

distribution function due to multiple Coulomb scattering (MCS) in matter. The procedures take into account the nuclear size effect and contribution of incoherent scattering on atomic electrons.

The paper is organized as follows. In Sec.2, we give the general relations and definitions used for description of multiple scattering of muons in the field of atoms. A mixed Monte Carlo approach to the MCS consideration is described in Sec.3. In Sec.4, contribution of incoherent scattering on atomic electrons and the multiple scattering in mixtures and compounds are discussed. Basic expressions of Moliere multiple scattering theory are given in Sec.5, whereas the equations of modified Moliere theory taking into account nuclear size effect are described in Sec.6. At the end of this section, we compare the angular distributions of muons obtained by Monte Carlo method and analytically. In the conclusion, the main results of the paper are summarized.

2 General relations and definitions

Differential cross section (per gram of matter) for scattering in Coulomb field of nuclei in the small angle approximation can be written as follows [7]:

$$d\sigma_0(\chi) = 8\pi N_{\text{Av}} \frac{Z^2}{A} \left(\frac{e^2}{pv}\right)^2 \frac{d\chi}{\chi^3} = 8\pi N_{\text{Av}} \frac{Z^2}{A} \left(\frac{r_e m_e}{p\beta}\right)^2 \frac{d\chi}{\chi^3}, \quad (1)$$

where N_{Av} is the Avogadro number, A is the atomic weight, p and v are momentum and velocity of the particle, respectively. In the second relation, classical electron radius r_e and electron mass m_e are utilised as natural units of distance and energy. Hereafter, whenever it does not cause misunderstanding, we assume $\hbar = c = 1$. For high-energy ($E \sim p$, $\beta \sim 1$) muon scattering on heavy target through small angles, the transverse momentum transferred to the particle $q = E\chi$, and practically coincides with the total 3-dimensional momentum transfer. The cross section may be re-written as:

$$d\sigma_0(q) = 8\pi N_{\text{Av}} \frac{Z^2}{A} (r_e m_e)^2 \frac{dq}{q^3}. \quad (2)$$

Noteworthy, in this ultrarelativistic regime the cross section depends only on transverse momentum and not on the particle energy. The integral cross section for scattering with transverse momenta greater than q is:

$$\sigma_0^{\text{int}}(q) = 4\pi N_{\text{Av}} \frac{Z^2}{A} \left(\frac{r_e m_e}{q}\right)^2. \quad (3)$$

Differential cross section for extended nuclei (taking into account also atomic screening) in the Born approximation may be described by means of formfactors:

$$d\sigma(q) = d\sigma_0(q) \left\{ (F_N - F_a)^2 + \frac{1}{Z} (1 - F_N^2) F_p^2 \right\}, \quad (4)$$

where $F_a(q)$, $F_N(q)$, and $F_p(q)$ are elastic atomic, nuclear, and proton formfactors, respectively. The second term in braces represents the (order-of-magnitude) correction for quasi-elastic processes (with excitation or disintegration of the nucleus), if incoherent scattering of the projectile on individual protons inside nucleus occurs. For hydrogen ($Z=1$) this term should be omitted.

Formfactors are normalised in such a way that $F(0) = 1$ and $F(\infty) = 0$. A big difference between the sizes of atom and nucleus allows, as a rule, to consider the influence of atomic and nuclear formfactor separately: in the region where F_a is essential, $F_N = 1$; on the contrary, when F_N appreciably deviates from the unit, F_a is negligibly small. Hence, in a wide range of momentum transfers (two - three orders of magnitude, depending on the substance), and, as a consequence, over 4 - 5 decades in interaction frequency determined by Eq.(3), individual scatters obey a simple Rutherford law.

The functional dependence of the formfactors is determined by the charge density distribution inside the object. For light and medium nuclei, a sufficiently good description may be reached on the basis of two-parameter distribution function suggested by Fermi. However, the use of accurate charge distributions entails serious computational difficulties and cannot be done in analytical form. Therefore, reasonable approximations are often used (for example, Gaussian or exponential distribution of charge density). For consideration of multiple scattering process, such approximations are justified by the fact that at moderate transferred momenta the same expansion can be written for all formfactors

$$F_N(q) \simeq 1 - (qR_N)^2 / 6, \quad (5)$$

where R_N is rms radius of charge distribution. An appreciable difference between different formfactors appears only in rare collisions with large q . Analytically, within the framework of Born approximation [8]

$$F_N(q) = \exp \left[-\frac{(qR_N)^2}{6} \right] \quad \text{and} \quad F_N(q) = \left[1 + \frac{(qR_N)^2}{12} \right]^{-2} \quad (6)$$

for Gaussian and exponential charge distributions, respectively. Rms-radii for practically all elements (and, moreover, for numerous isotopes) can be found elsewhere (e.g., see the compilation in Ref.[9]). For light and medium nuclei,

the A -dependence of R_N may be parameterized as

$$R_N = 1.27A^{0.27} \text{ fm} \quad \text{or} \quad q_N = 1/R_N = 155A^{-0.27} \text{ MeV}. \quad (7)$$

For proton, $R_p = 0.85 \text{ fm}$, and $q_p = 232 \text{ MeV}$.

The important parameter in consideration of multiple scattering phenomenon is a so-called characteristic value q_c of transverse momentum, which determines on the average one scatter with $q > q_c$ at a given layer thickness $X(\text{g}/\text{cm}^2)$:

$$q_c^2 = 4\pi N_{\text{Av}} \frac{Z^2}{A} (r_e m_e)^2 X. \quad (8)$$

Sometimes, the following regions are distinguished in the scattering process: multiple scattering ($q \ll q_c$, numerous scatters), plural scattering (several, but few, scatters with $q \sim q_c$), and single scattering (low probability scatters with $q \gg q_c$); in the latter domain, scattering angle distribution function approaches the behaviour of the differential cross section.

Statistical consideration of multiple scattering is appropriate when $q_c \gg 1/R_a$, where R_a is the effective radius of the atomic electron charge distribution:

$$R_a = 1/q_a = \frac{183Z^{-1/3}}{2.718m_e}. \quad (9)$$

Hence, the applicability of theory is usually limited to thickness of layers:

$$X \gg 4 \cdot 10^{-4} A/Z^{4/3} \text{ g}/\text{cm}^2. \quad (10)$$

3 Monte Carlo approach

The idea of MCS consideration by means of a mixed Monte Carlo technique (see, e.g., Ref.[10]) consists in the separation of multiple scattering through small angles, or with small transferred momenta (which are treated in Gaussian approximation), and of scatters in the region of large q , which are simulated explicitly. This approach can be conveniently used for calculations with accurate cross section in high q region (in particular, including nuclear formfactors). The boundary q_b between these two domains has to satisfy the following inequalities:

$$q_a \ll q_b \ll q_N; \quad q_b \leq q_c. \quad (11)$$

The first of these two conditions ensures Rutherford behaviour of the cross section around q_b , while the second one provides the regime of plural or multiple interactions for scatters that are simulated individually.

In order to calculate the rms-deviation for small angle scatters with $q < q_b$, which are treated in a "continuous" way, the following integral has to be evaluated:

$$\int_0^{q_b} [1 - F_a(q)]^2 \frac{dq}{q}. \quad (12)$$

A similar integral comes into cross section formulae for many electromagnetic interaction processes (for example, radiation logarithm in the bremsstrahlung), and a ready result of work [11] can be used. In the frame of the Thomas-Fermi model, one can find for the "restricted" value of squared transverse momentum accumulated in the layer X of matter:

$$\langle Q^2 \rangle_{\text{rstr}} = 8\pi N_{Av} (r_e m_e)^2 \frac{Z^2}{A} X \left[\ln K Z^{-1/3} + \ln \frac{q_b}{m_e} - 1 \right], \quad (13)$$

where $K=183$. Using Eq.(8) and Eq.(9), we can re-write the latter relation as

$$\langle Q^2 \rangle_{\text{rstr}} = 2q_c^2 \ln \frac{q_b}{q_a}. \quad (14)$$

For light and medium elements, Thomas-Fermi model of the atom does not provide high accuracy. For example, for hydrogen it is necessary to take $K=202.4$; the values of K for various elements calculated with Hartree-Fock model may be found elsewhere [12].

Random scatters with $q > q_b$ are simulated by means of a usual technique, with the mean free path defined by the integral cross section (3). Random q_ζ are sampled as

$$q_\zeta = q_b / \sqrt{\zeta}, \quad (15)$$

where ζ is a random number with a uniform distribution between 0 and 1; q_ζ is accepted with a probability equal to the combined nuclear formfactor \mathcal{F}_N^2 (including elastic and quasielastic terms):

$$P(q_\zeta) = \mathcal{F}_N^2 = F_N^2 + \frac{1}{Z} (1 - F_N^2) F_p^2. \quad (16)$$

Again, similar to Eq.(4), only the first term remains for hydrogen (with nuclear formfactor equal to that of proton).

Although the consistency of the approach based on the partition of individual scatters into "continuous" ($q < q_b$) and "discrete" ($q > q_b$) parts is almost obvious, we have performed comparative calculations for different thicknesses of absorber (1 cm and 100 cm iron), each with two substantially different values of q_b (0.1 and 1 MeV for thin absorber, 1 and 10 MeV for thick layer); 10^6 muons for the lower value of q_b and 10^8 for the higher one have been traced. Noteworthy, the number of simulated individually scatters (per muon) varies as $1/q_b^2$ (see Eq.(3)), and hence it was 100 times different (about 15 per layer for the higher value of the threshold and ~ 1500 for the lower one).

Differential distributions of events in the value of accumulated transverse momentum Q are shown in Figs.1 and 2 for 1 cm and 100 cm iron targets, respectively. A big difference between calculation results for point-like and finite-size nucleus is obvious already for 1 cm layer. On the other hand, the results obtained with different boundary values q_b agree within the statistical accuracy in the whole range of angular deviations.

Monte Carlo approach allows to easily probe different models of the nuclear formfactor. In Fig.3, comparison of calculation results obtained for several versions of the formfactor is given. Integral distributions in Q (i.e. probabilities of the deflection at angles greater than Q/E) after passing 100 cm iron layer are presented. Solid curves (bottom to top) in the figure correspond to: Gaussian charge distribution in nucleus, incoherent scattering on protons being neglected (i.e., the second term in Eq.(16) is omitted); Gaussian charge distribution both in nucleus and in proton; exponential distribution for nucleus and proton; exponential model for nucleus with proton taken as a point-like object ($F_p=1$). With the exception of unrealistic extreme cases, calculation results are not very sensitive to the choice of a specific formfactor model. At the same time, the difference with the calculations performed for a point-like nucleus (dashed curve in the figure) is very big, and reaches the orders of magnitude in the probability of large deflections.

The total average value of squared transverse momentum accumulated in the layer can be obtained, if we add the contribution of large deflections ($q > q_b$) to the restricted value given by Eq.(14). For Gaussian charge distribution, such evaluation can be easily performed analytically:

$$\langle Q^2 \rangle = 2q_c^2 \left[\ln \frac{1.2978q_N}{q_a} + \frac{1}{2Z} \ln \left(1 + \frac{q_p^2}{q_N^2} \right) \right], \quad (17)$$

where q_N , q_p , q_c , and q_a are defined by Eqs.(7)-(9). The average contribution of quasielastic processes (the second term in brackets) is small even for light elements; for example, in carbon the rms-deviation increases by only 1%. However, these interactions have to be taken into account for adequate description of the distribution function in the tail region (see Fig.3).

For three-dimensional calculations, when both angular deviation and lat-

eral displacement of muon are of interest, the restricted contribution (of $q < q_b$) can also be calculated in a Gaussian approximation, but taking into account the well-known correlation between the angle and the displacement [13].

4 Atomic electron contribution; mixtures and compounds

Contribution of incoherent scattering on atomic electrons is often taken into account by means of a substitution of Z^2 by $Z(Z + 1)$ in basic relations (for differential cross section, some parameters of the theory, etc.). However, this substitution is rather inaccurate, since, firstly, the cross section at small angles (and low momenta) is determined in this case by the inelastic atomic formfactor (with different q -dependence and different characteristic radius of the atom). Secondly, due to light electron mass, kinematics of the process (in laboratory frame) appreciably changes. That leads to the appearance of the upper limit on transverse momentum and on deflection angle, and to an appreciable probability to loose large fraction of muon energy in a single collision. Of course, target size corrections for scattering on electrons are irrelevant.

Consideration of kinematics of muon scattering on a free electron gives the following expression for the transverse momentum q

$$q = \sqrt{2m_e T(1 - T/T_m)}, \quad (18)$$

where T and T_m are kinetic energy transferred to the electron (initially at rest) in the collision and the maximal value of this energy:

$$T_m = 2m_e p^2 / (m_e^2 + m_\mu^2 + 2m_e E). \quad (19)$$

The accumulated squared transverse momentum in the layer X may be evaluated similar to Eq.(13), combining the contribution of low- q region (where the inelastic atomic formfactor is important) and of high- q domain. In the latter case, $\langle Q^2 \rangle$ is easily calculated by means of the convolution of the squared value of q (Eq.(18)) and the differential cross section of knock-on electron production. In this way, we obtain the following relation:

$$\langle Q^2 \rangle = 8\pi N_{Av} \frac{Z}{A} X (r_e m_e)^2 \left[\ln \left(K' Z^{-2/3} \sqrt{\frac{2T_m}{m_e}} - \frac{7}{4} \right) \right]. \quad (20)$$

Within the Thomas-Fermi model, $K'=1429$; an accurate value for hydrogen is $K'=446$. Small corrections which correspond to spin terms in the cross section of muon-electron scattering are omitted for simplicity.

Rare catastrophic collisions with large energy transfers are also included in

$\langle Q^2 \rangle$ calculations (Eq.(20)) on the average. For simulation of muon transport in thick layers, such collisions are usually treated separately (with explicit simulation of kinematic variables). The average accumulated Q^2 in collisions with energy transfers less than a certain cut T_c ($T_c \leq T_m$) is given by

$$\langle Q^2 \rangle_{\text{rstr}} = 8\pi N_{\text{Av}} \frac{Z}{A} X(r_e m_e)^2 \left[\ln \left(K' Z^{-2/3} \sqrt{\frac{2T_c}{m_e}} \right) - 1 - \frac{T_c}{T_m} + \frac{T_c^2}{4T_m^2} \right]. \quad (21)$$

Multiple scattering on the electrons represents only a correction to the scattering on nuclei, and maximal transverse momenta and deflection angles are small. Therefore it seems justified to introduce this correction on the basis of a Gaussian approximation (for example, as an addition of contribution given by Eq.(21) to the restricted value of accumulated Q^2 on nuclei defined by Eq.(13)). Such procedure allows to avoid double counting of the collisions with energy transfers $T > T_c$, which will appear if multiple scattering process and knock-on electron production are simulated incoherently.

As a general prescription, for calculation of multiple scattering in mixtures or compounds, the differential cross sections Eq.(4) for elements have to be averaged with weights W_i corresponding to relative mass abundance of individual entries.

Within the framework of a mixed Monte Carlo approach described above, this leads to: (i) summation of restricted accumulated Q^2 -values with weights W_i ; (ii) description of the cross section in the intermediate region ($q_a \ll q \ll q_N$) with the average parameter $\langle Z^2/A \rangle$ (and, hence, of the integral cross section for $q > q_b$ with the same factor); (iii) averaging of the acceptance function Eq.(16) for sampling of random momenta $q_c > q_b$:

$$P(q_c) = \sum_{i=1}^n W_i \frac{Z_i^2}{A_i} \left\{ F_{N_i}^2 + \frac{1}{Z_i} (1 - F_{N_i}^2) F_p^2 \right\} / \sum_{i=1}^n W_i \frac{Z_i^2}{A_i}. \quad (22)$$

Here, $F_{N_i}(q_c)$ denotes the elastic nuclear formfactor for the i -th element of the mixture. For hydrogen, the expression in braces reduces to the first term (see also comments after Eqs.(4) and (16)). Similarly, the contribution of the scattering on atomic electrons is determined by the weighted sum of partial contributions defined by Eqs.(20) or (21), for total or restricted (with $T < T_c$) accumulated Q^2 values, respectively.

5 Moliere's equations

In this section, we give the main equations of the Moliere's multiple scattering theory where the nucleus is treated as a point-like charge.

Let $f(\theta, t)$ be spatial-angle distribution function, i.e. for small-angle approximation $f(\theta, t)$ it is the number of charged particles in the angular interval of polar angle $\theta \div \theta + d\theta$ after traversing a thickness of t . Moliere solved the transport equation for determination of $f(\theta, t)$ and obtained the general expression for angular distribution function as a following:

$$f(\theta, t) = \frac{1}{2\pi} \int_0^\infty \xi d\xi J_0(\xi\theta) e^{\Omega(\xi, t)}, \quad (23)$$

where $J_0(\xi\theta)$ is the Bessel function of order 0. For a homogeneous scatterer without energy loss, we have

$$\Omega(\xi) = 2\pi t \int_0^\infty \chi d\chi [J_0(\xi\chi) - 1] W(\chi), \quad (24)$$

where

$$W(\chi) = N\sigma(\chi). \quad (25)$$

Here $N = N_{Av}\rho/A$ (ρ is density of the scatterer in g/cm^3) is the number of scattering atoms per unit volume, with differential cross-section $\sigma(\chi)$ each.

The scattering of relativistic particle by an atom is determined by a modified Rutherford law

$$\sigma(\chi) = \sigma_{\text{Ru}}(\chi)\Psi(\chi)\mathcal{F}_N^2(\chi), \quad (26)$$

where $\sigma_{\text{Ru}}(\chi)$ is Rutherford cross-section for scattering by point-like charge, $\Psi(\chi)$ is a function which takes into account the screening of the nuclear Coulomb field by atomic electrons, and $\mathcal{F}_N(\chi)$ is the nuclear formfactor Eq.(16). In Moliere's theory, the following approximations are used: $\mathcal{F}_N^2(\chi)=1$,

$$\sigma_{\text{Ru}}(\chi) = 4 \frac{Z^2 e^4}{p^2 \chi^4}, \quad (27)$$

and the screening function is

$$\Psi(\chi) = \chi^4 / (\chi^2 + \chi_\alpha^2)^2, \quad (28)$$

where the screening angle is

$$\chi_\alpha^2 = \chi_0^2 (1.13 + 3.76(Z\alpha)^2), \quad (29)$$

$$\alpha = 1/137, \quad \text{and} \quad \chi_0 \simeq \frac{1.13}{137} Z^{1/3} m_e/p.$$

In his original paper, Moliere used the variables

$$\vartheta = \theta/\chi_c\sqrt{B} \quad \text{and} \quad \eta = \xi\chi_c\sqrt{B}, \quad (30)$$

where the characteristic angle χ_c is defined as

$$\chi_c^2 = \frac{4\pi NtZ^2e^4}{p^2}. \quad (31)$$

Here t is measured in cm, and B equals to the solution of the transcendental equation

$$B - \ln B = 1 - 2C + \ln(\chi_c^2/\chi_\alpha^2) \quad (32)$$

($C = 0.5772$ is Euler constant). Then the expression for the angular distribution function can be written as

$$f(\theta, t)\theta d\theta = f_M(\vartheta, B)\vartheta d\vartheta, \quad (33)$$

where

$$f_M(\vartheta, B) = \int_0^\infty \eta d\eta J_0(\eta\vartheta) e^{-\eta^2/4} \exp\left(\frac{\eta^2}{4B} \ln \frac{\eta^2}{4}\right).$$

Moliere's expansion method is to consider the term $[\eta^2 \ln(\eta^2/4)]/4B$ as a small parameter; then the exponent can be expanded to second order terms

$$f_M(\vartheta, B) = f_M^{(0)}(\vartheta) + f_M^{(1)}(\vartheta)/B + f_M^{(2)}(\vartheta)/B^2 + \dots, \quad (34)$$

where

$$f_M^{(n)}(\vartheta) = \frac{1}{n!} \int_0^\infty \eta d\eta J_0(\vartheta\eta) e^{-\eta^2/4} \left[\frac{\eta^2}{4} \ln \frac{\eta^2}{4}\right]^n. \quad (35)$$

The first two functions $f^{(n)}$ have simple analytical forms:

$$f_M^{(0)}(\vartheta) = 2e^{-\vartheta^2}, \quad f_M^{(1)}(\vartheta) = 2e^{-\vartheta^2}(\vartheta^2 - 1) \left[E_1(\vartheta^2) - \ln \vartheta^2 \right] - 2(1 - 2e^{-\vartheta^2}), \quad (36)$$

where $E_1(\vartheta^2)$ is the exponential integral. The Moliere's theory is valid for $B \geq 4.5$ and $\chi_c^2 B < 1$ [2],[3].

6 Modified Moliere theory

The effect of nuclear size can be evaluated using a suitable formfactor $\mathcal{F}_N(\chi)$ in Eq.(26). The general method to take into account nuclear effects for arbitrary charge distribution in nucleus has been suggested by Cooper and Rainwater [4]. The Gaussian approximation of nucleus and protons formfactors was regarded in paper [5]. In this case, assuming that $q_p \gg q_N$ one can re-write the Eq.(16) as

$$\mathcal{F}_N^2(\chi) = \left(1 - Z^{-1}\right) e^{-\chi^2/a_A^2} + Z^{-1} e^{-\chi^2/a_p^2}, \quad (37)$$

where (see Eq.(7) and Eq.(16))

$$a_A^2 = 3q_N^2/E^2 \quad \text{and} \quad a_p^2 = 3q_p^2/E^2.$$

Using Eqs.(24)-(28) and Eq.(37), the function $\Omega(\xi)$ can be written as

$$\Omega(\xi) = 2\chi_c^2 \int_0^\infty \frac{\chi d\chi}{(\chi^2 + \chi_c^2)^2} [J_0(\xi\chi) - 1] \left[\left(1 - Z^{-1}\right) e^{-\chi^2/a_A^2} + Z^{-1} e^{-\chi^2/a_p^2} \right]. \quad (38)$$

This integral can be evaluated analytically, and we have

$$\Omega(\xi) = -\frac{\eta^2}{4} + \frac{1}{B} \left[\left(1 - Z^{-1}\right) D_A(\eta, \tau_A^2) + Z^{-1} D_p(\eta, \tau_p^2) \right], \quad (39)$$

where

$$D(\eta, \tau^2) = \frac{\eta^2}{4} \left[\ln \frac{\eta^2}{4} + E_1\left(\frac{\eta^2 \tau^2}{4}\right) \right] + \frac{1}{\tau^2} \left[C + \ln \frac{\tau^2 \eta^2}{4} + 1 - e^{-\eta^2 \tau^2/4} + E_1\left(\frac{\eta^2 \tau^2}{4}\right) \right], \quad (40)$$

and

$$\tau^2 = a^2/\chi_c^2 B.$$

Then angular distribution function $\tilde{f}_M(\vartheta, \tau)$ is

$$\tilde{f}_M(\vartheta, \tau) = \int_0^\infty \eta d\eta J_0(\eta, \vartheta) e^{-\eta^2/4} \exp \left\{ \frac{1}{B} \left[\left(1 - Z^{-1}\right) D(\eta, \tau_A^2) + Z^{-1} D(\eta, \tau_p^2) \right] \right\}. \quad (41)$$

The exponent in Eq.(41) may be expanded in a series, and we obtain

$$\tilde{f}_M(\vartheta, \tau) = \sum_{n=0}^{\infty} \frac{1}{B^n} \tilde{f}_M^{(n)}(\vartheta, \tau) \approx \tilde{f}_M^{(0)}(\vartheta) + \frac{1}{B} \tilde{f}_M^{(1)}(\vartheta, \tau) + \dots, \quad (42)$$

where

$$\tilde{f}_M^{(n)}(\vartheta, \tau) = \frac{1}{n!} \int_0^{\infty} \eta d\eta J_0(\eta, \vartheta) e^{-\eta^2/4} \left[(1 - Z^{-1}) D(\eta, \tau_A^2) + Z^{-1} D(\eta, \tau_p^2) \right]^n. \quad (43)$$

At $n = 0$ and 1 , the integrals Eq.(43) equal to ¹

$$\tilde{f}_M^{(0)}(\vartheta) = 2 e^{-\vartheta^2}, \quad \tilde{f}_M^{(1)}(\vartheta, \tau) = 2 e^{-\vartheta^2} \left[2 + (1 - Z^{-1}) G(\vartheta, \tau_A^2) + Z^{-1} G(\vartheta, \tau_p^2) \right], \quad (44)$$

where

$$G(\vartheta, \tau^2) = \frac{1}{\tau^2} (C + 1 + \ln \tau^2) + \kappa^2 \left(\frac{\vartheta^2}{\kappa^2} - 1 \right) \left[Ei\left(\frac{\vartheta^2}{\kappa^2}\right) - \ln \vartheta^2 \right] - \kappa^2 e^{\vartheta^2/\kappa^2}, \quad (45)$$

and $\kappa^2 = 1 + 1/\tau^2$ (in Ref.[5] the coefficient κ^2 is missing in the last term).

The integral angular distribution $P(\vartheta, t)$ is

$$P(\vartheta, t) = \sum_{n=0}^{\infty} \frac{1}{B^n} \int_{\vartheta}^{\infty} \tilde{f}_M^{(n)}(\vartheta', \tau) \vartheta' d\vartheta' \approx P^{(0)}(\vartheta) + P^{(1)}(\vartheta, \tau) + \dots, \quad (46)$$

where

$$P^{(0)}(\vartheta) = e^{-\vartheta^2}, \quad P^{(1)}(\vartheta, \tau) = \frac{1}{B} \left[(1 - Z^{-1}) Q(\vartheta, \tau_A^2) + Z^{-1} Q(\vartheta, \tau_p^2) \right], \quad (47)$$

and

$$Q(\vartheta, \tau^2) = e^{-\vartheta^2} \left\{ \frac{\tau^2 + C + 1 + \ln \tau^2}{\tau^2} + (\kappa^2 - 1) \left[R_1(\vartheta, \tau^2) + R_2(\vartheta, \tau^2) \right] \right\}. \quad (48)$$

The functions R_1 and R_2 are

$$R_1(\vartheta, \tau^2) = e^{\vartheta^2} \left[Ei\left(-\frac{\vartheta^2}{1 + \tau^2}\right) - Ei(-\vartheta^2) \right],$$

¹ Note that integrals with $E_1(\eta^2\tau^2/4)$ can be evaluated using derivation over the parameter τ^2 .

$$R_2(\vartheta, \tau^2) = \left(\frac{\vartheta^2}{\kappa^2 - 1} - 1 \right) \left[Ei \left(\frac{\vartheta^2}{\kappa^2} \right) - \ln \vartheta^2 \right] - \kappa^2 e^{\vartheta^2/\kappa^2}.$$

The function $\tilde{f}_M(\vartheta, \tau) \rightarrow f_M(\vartheta)$ at $\langle R_N^2 \rangle$ and $\langle R_p^2 \rangle \rightarrow 0$. On the other hand, $\tau^2 \rightarrow \infty$ at $t \rightarrow 0$ also. So, the angular distribution of relativistic particles should be similar to Moliere distribution after passing through the small thicknesses of matter. However, even for thin layers the distribution function appreciably deviates from the Moliere law at large deflection angles ($\theta > q_N/E$), and tends to the cross section behaviour Eq.(26) with formfactors. The expansions to the first order terms of Eq.(42) and Eq.(46) are valid up to $\tau_A^2 \geq 0.2$. For thick layer of matter (τ_A^2 and $\tau_p^2 \ll 1$), the asymptotic of Eq.(42) is Gaussian [5]:

$$\tilde{f}_M(\vartheta, \tau) \simeq \int_0^\infty J_0(\eta\vartheta) e^{-\mu\eta^2/4} \eta d\eta = \frac{2}{\mu} e^{-\vartheta^2/\mu}, \quad (49)$$

where

$$\mu = 1 - \frac{1}{B} \left[2 - C - \ln \tau_A^2 - Z^{-1} \ln \frac{\tau_p^2}{\tau_A^2} \right]. \quad (50)$$

If the mixture of n different scatterers is present, the characteristic angle χ_c is given by

$$\chi_c^2 = \frac{4\pi e^4}{p^2} N_{Av} \rho t \frac{\sum_{i=1}^n w_i Z_i^2}{\sum_{i=1}^n w_i A_i}, \quad (51)$$

and the integral angular distribution function $P(\vartheta, t)$ is defined by

$$P(\vartheta, t) = \frac{\sum_{i=1}^n w_i Z_i^2 P_i(\vartheta, t)}{\sum_{i=1}^n w_i Z_i^2}, \quad (52)$$

where the subscript i denotes the atomic species and weight w_i is proportional to the number of atoms of the i -th element in the mixture.

The integral angular distributions on nuclei as a function of the transverse momentum Q calculated by the mixed Monte Carlo technique and analytically Eq.(46) are shown in Fig.4 (iron targets of 1 cm and 100 cm) and in Fig.5 (water thickness of 1000 cm). The results are in good agreement. Moliere angular distributions are shown also for comparison. A minor difference between analytical and Monte Carlo calculations in the tails of the curves is conditioned by a different choice of the proton formfactor (Gaussian charge distribution with $R_p = 0.80$ fm in analytical evaluation and exponential one with $R_p = 0.85$ fm in Monte Carlo simulation).

7 Conclusions

A high-energy muon is capable to cross very thick layers of material and its de Broglie wave is comparable with nuclear dimensions. Hence, the probability of scatters with impact parameter of the order of nuclear radius (scatters with large angles) is not small. For such interactions, the law of single scattering has to be modified significantly to take into account the finite size of charge distribution in the nuclei. Nuclear size effects can be described by multiplying the Rutherford cross section by a nuclear formfactor \mathcal{F}_N^2 , which goes to 1 for large impact parameters and vanished at very large transverse momenta.

We have presented two methods for calculating the multiple scattering distribution for muons traversing a thick scatterer. The mixed Monte Carlo technique and modified Moliere's theory of MCS take into account the nuclear size effect. Parametrisation of A -dependence of rms-radii for light and medium nuclei is given. The results of two methods are in good agreement, and show that the muon angular distribution is similar to Moliere distribution after passing through small thickness of material and moderate deflection angles. However at large thickness of scatterer, the angular distribution is drastically changed by the influence of the nuclear formfactor. So, in this case the Moliere theory heavily overestimates the probability of large angle deflections. Contribution of incoherent scattering on atomic electrons is also correctly taken into account.

A necessity of taking into account nucleus size effect as well as incoherent scattering on atomic electrons when describing the muon scattering at large angles in thick matter layers is shown. Neither Gaussian approximation of multiple scattering distribution nor Moliere theory can be used for accurate description of high-energy muon transport in a wide range of the thicknesses of material.

Acknowledgements

Authors are indebted to A.A. Petrukhin for stimulating interest and critical comments. We acknowledge helpful discussions with V.L. Matushko. The work was supported in part by Russian Federal Program "Integratsiya" (project A-0100) and RFBR grant 99-02-18374.

References

- [1] W.T. Scott, Rev. Mod. Phys. 35 (1963) 231.
- [2] G.S. Moliere, Naturforsch. 2a (1947) 133; 3a (1948) 78; 10a (1955) 177.
- [3] H.A. Bethe Phys. Rev., 89 (1953) 1256.
- [4] L.N. Cooper, J. Rainwater Phys. Rev., 97 (1955) 492.
- [5] I.S. Baishev, N.V. Mokhov and S.I. Striganov, Sov. Journal of Nucl. Phys. 42 (1985) 1175.
- [6] U. Fano Phys. Rev. 93 (1954) 117.
- [7] B. Rossi, High Energy Particles, New York, (1952).
- [8] R. Hofstadter, Rev. Mod. Phys. 28 (1952) 214.
- [9] H. de Vries et al., Atomic Data and Nuclear Data Tables 36 (1987) 495.
- [10] J.M. Fernandez-Varea et al., Nucl. Instrum. and Meth., B 73 (1993) 447.
- [11] H.A. Bethe, Proc. Cambr. Phil. Soc., 30 (1934) 524.
- [12] S.R. Kelner et al., Physics of Atomic Nuclei, 62, (1999) 1894.
- [13] Particle Data Group. Review of Particle Physics, Section 23.3; EPJ, C15 (2000) 166.

Figure Captions

Fig.1: Differential distribution in accumulated transverse momentum for muons after passing iron of 1 cm. Dashed curves, open circles: point-like nucleus. Solid curves, dark points: calculations taking into account the nuclear formfactor. Curves are calculated with $q_b=1$ MeV (10^8 events), the points correspond to $q_b=0.1$ MeV (10^6 events).

Fig.2: The same as in Fig.1 but for iron target of 100 cm. In this case, the values of q_b in simulation were 10 MeV and 1 MeV, respectively.

Fig.3: Integral distributions in the value of accumulated transverse momentum for muons after passing iron layer of 100 cm, calculated with different models of the nucleus (see the text).

Fig.4: Integral distributions in the value of accumulated transverse momentum for muons after passing iron layers of 1 cm and 100 cm calculated by the mixed Monte Carlo technique (open circles for point-like nucleus and dark points for finite nuclei) and analytically (solid curves are result of Moliere theory and dashed curves are calculations taking into account the nuclear size effect).

Fig.5: Integral distributions in the value of accumulated transverse momentum for muons after passing water layer of 1000 cm calculated by the mixed Monte Carlo technique (dark points for point-like nucleus, open circles for finite nuclei and stars is a result of calculations, taking into account the nuclear formfactor and electron contribution) and analytically (solid curves are result of Moliere theory and dashed curves are calculations taking into account the nuclear size effect).

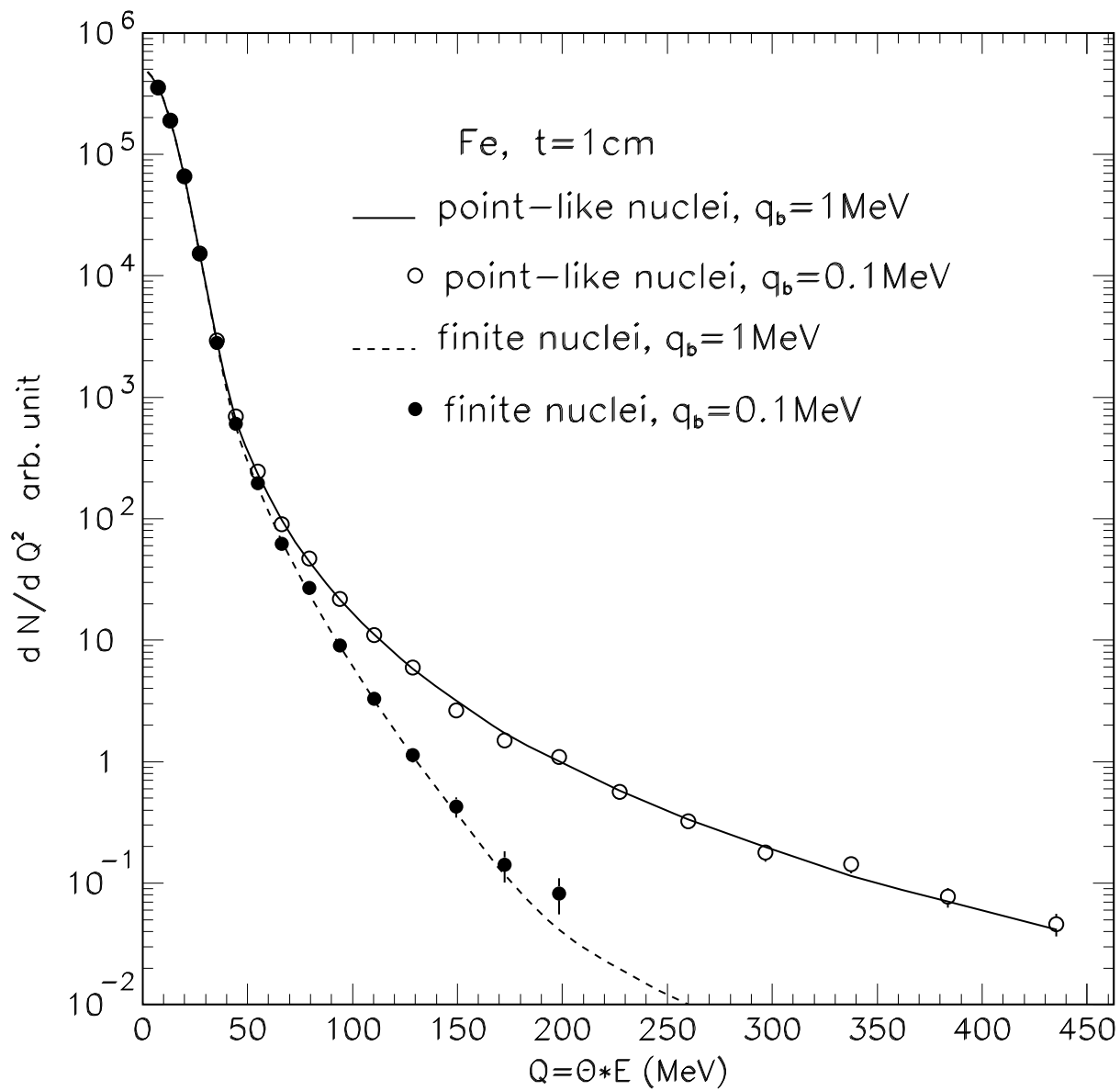


Fig. 1

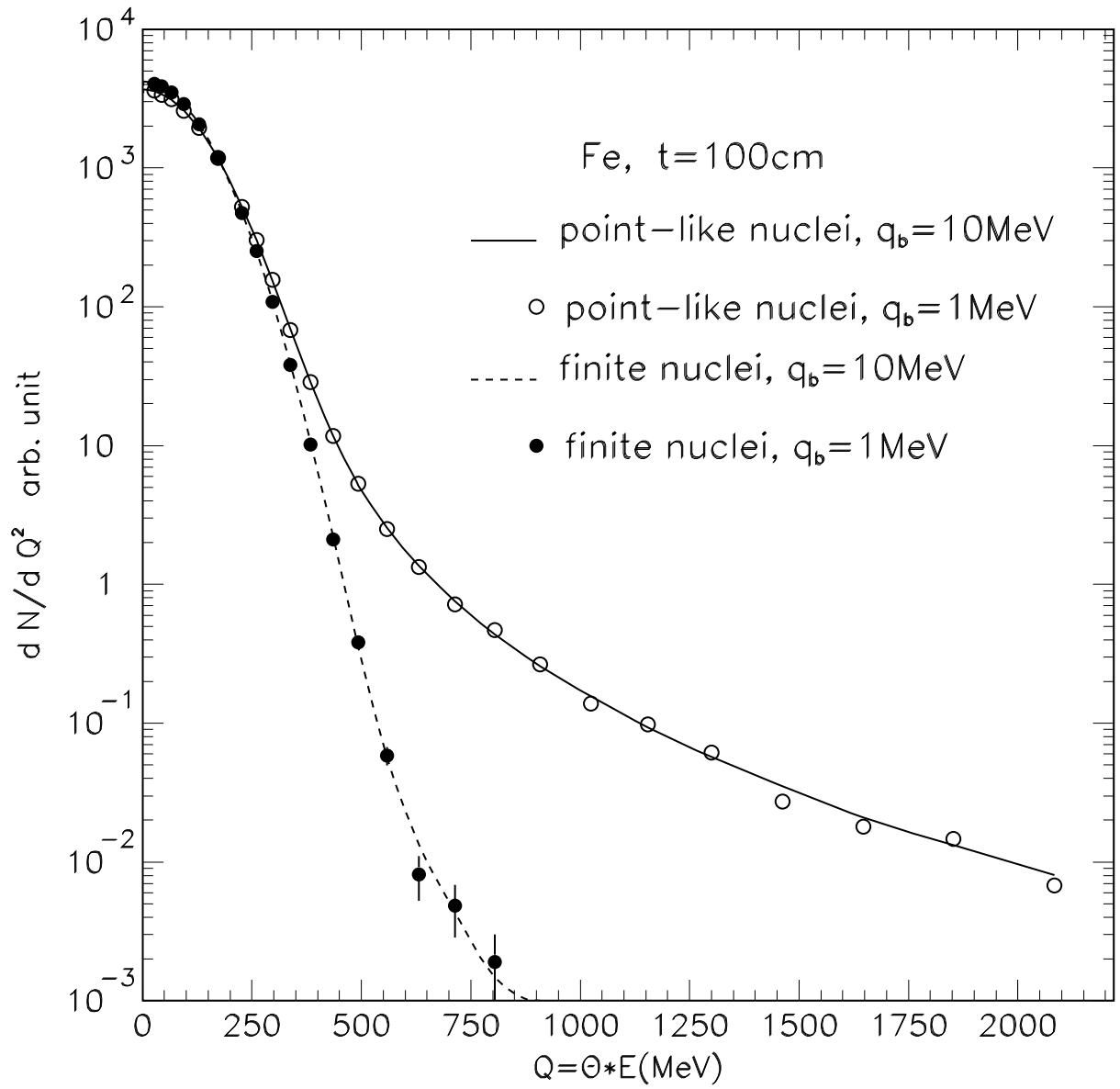


Fig. 2

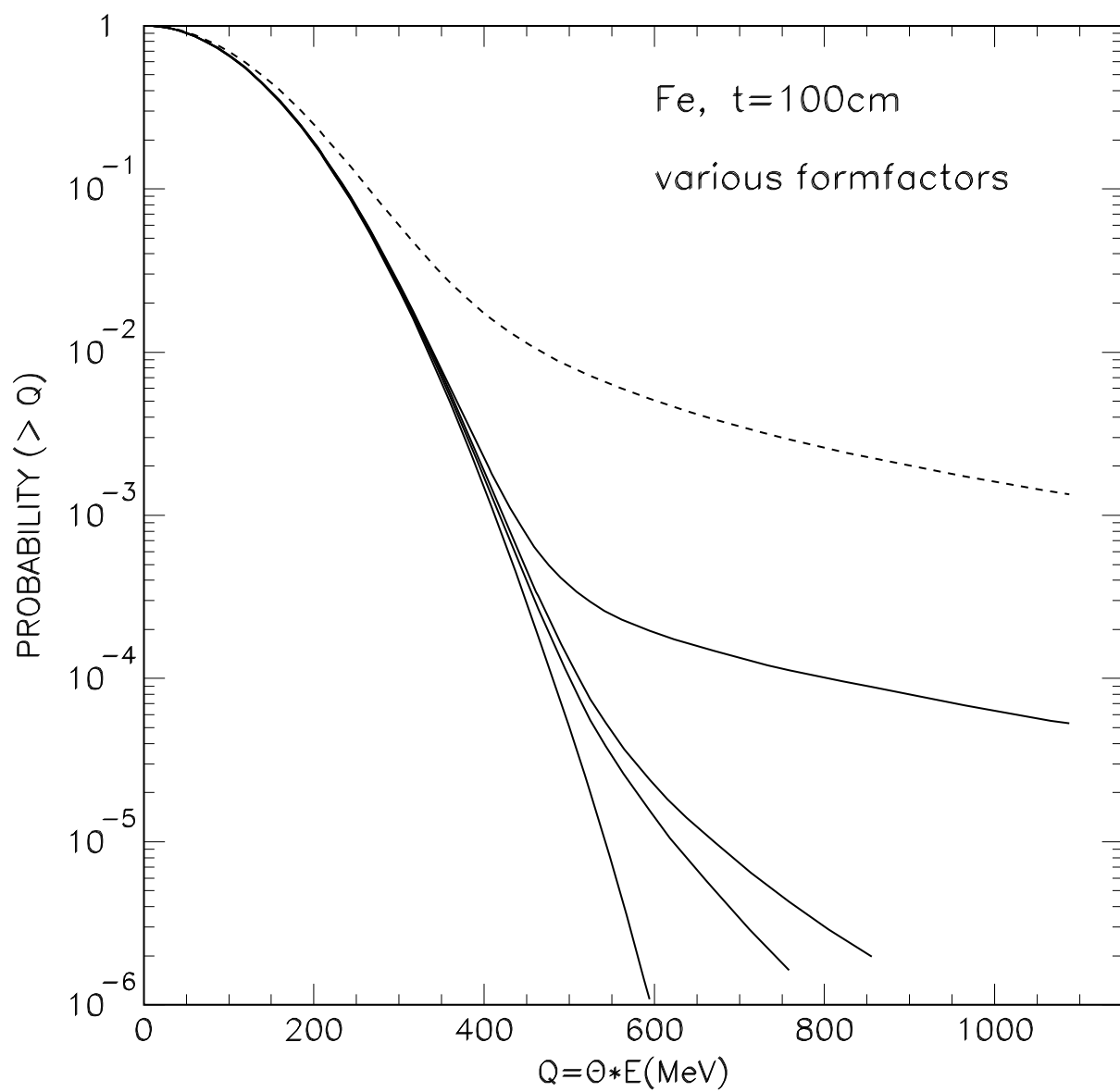


Fig. 3

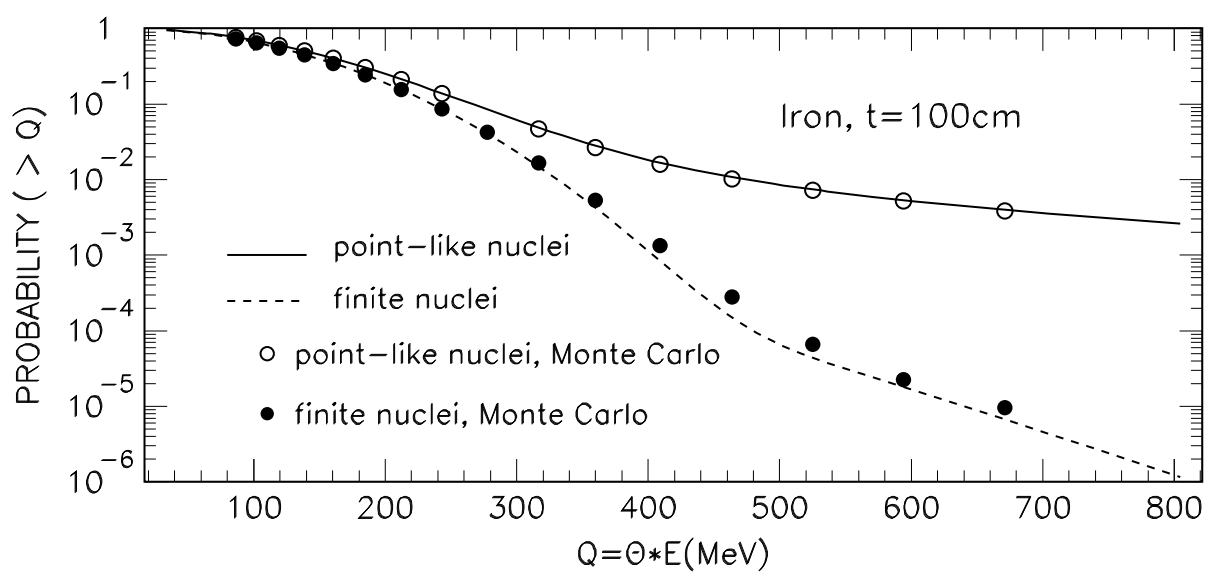
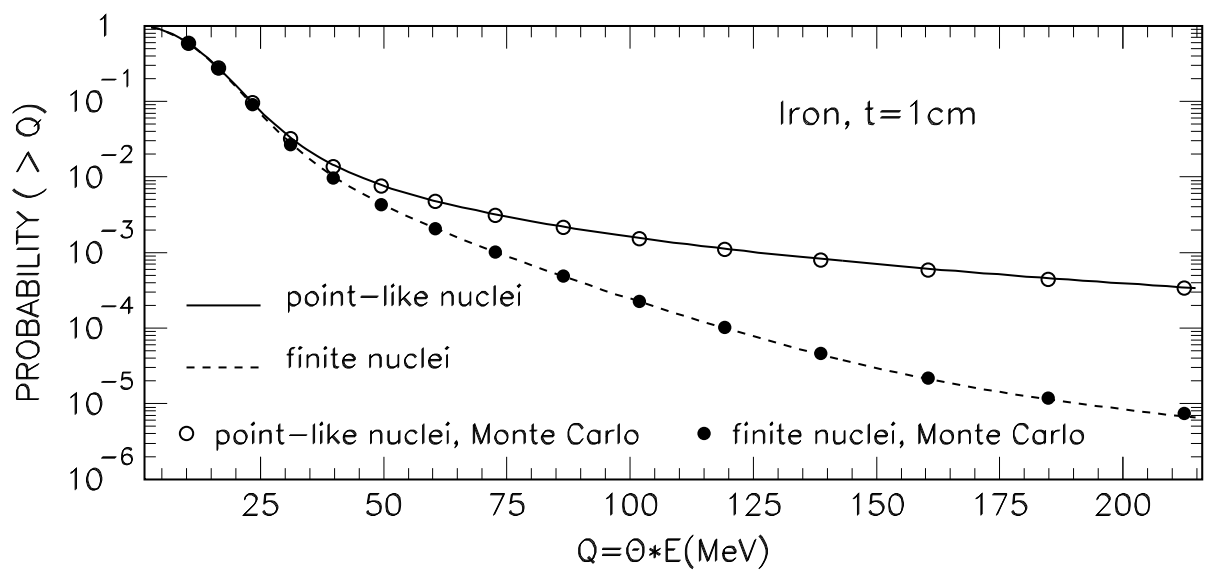


Fig. 4

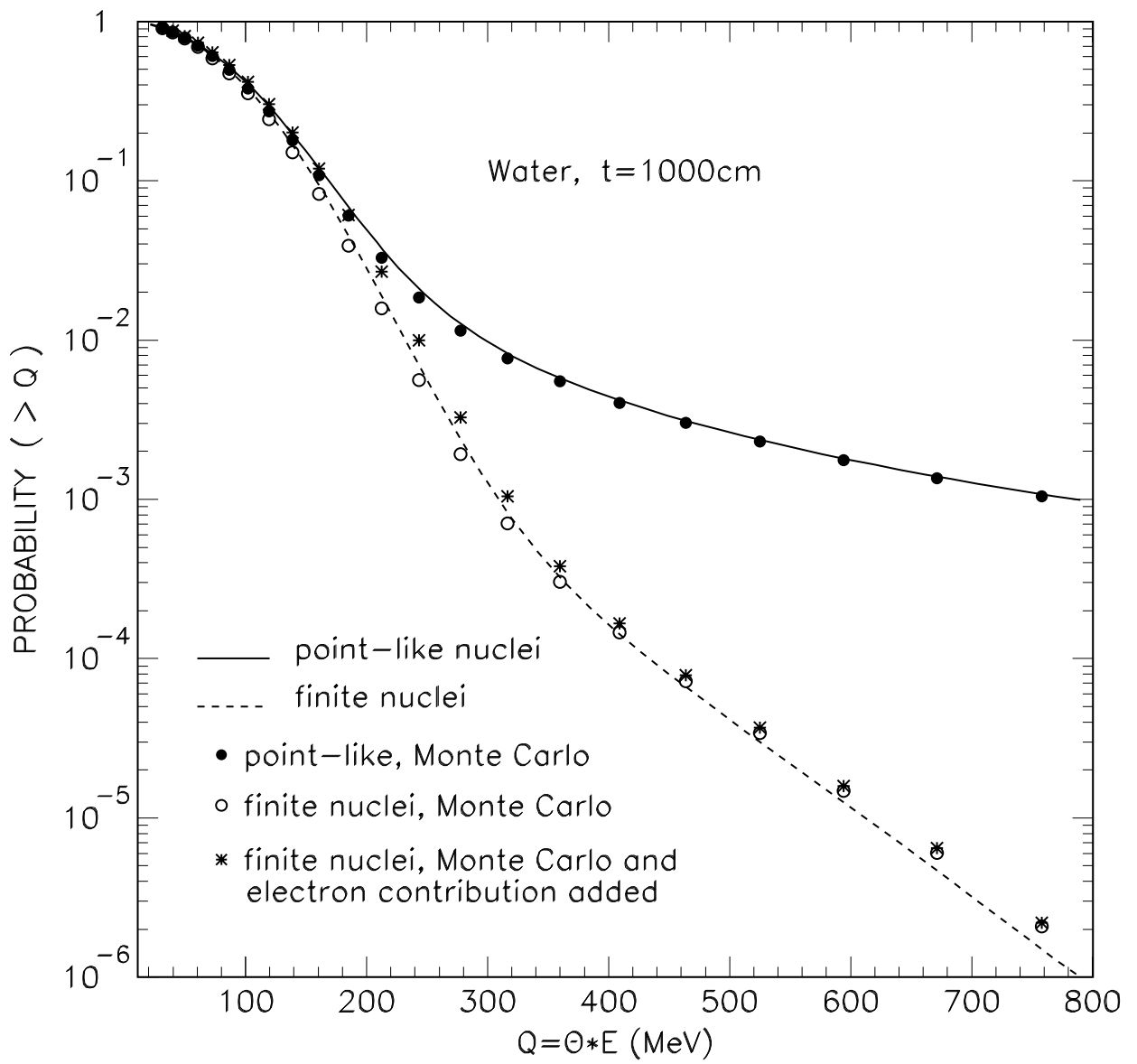


Fig. 5